

INTRIGUING INVARIANTS OF CENTERS OF ELLIPSE-INScribed TRIANGLES

MARK HELMAN, RONALDO GARCIA, AND DAN REZNIK

ABSTRACT. We describe invariants of centers of ellipse-inscribed triangle families with two vertices fixed to the ellipse boundary and a third one which sweeps it. We prove that: (i) if a triangle center is a fixed linear combination of barycenter and orthocenter, its locus is an ellipse; (ii) and that over the family of said linear combinations, the centers of said loci sweep a line; (iii) over the family of parallel fixed vertices, said loci rigidly translate along a second line. Additionally, we study invariants of the envelope of elliptic loci over combinations of two fixed vertices on the ellipse.

Keywords Ellipse, Locus, Invariant, Envelope, Limaçon.

MSC 53A04 and 51M04 and 51N20

1. INTRODUCTION

We describe a few intriguing invariants displayed by triangles centers [12] of ellipse-inscribed triangle families $\mathcal{T}(t) = V_1V_2P(t)$: V_1, V_2 are fixed on the boundary of an ellipse \mathcal{E} , and $P(t)$ sweeps said boundary. One readily observes that the locus of classic triangle centers such as the bary-, circum-, and orthocenter (denoted $X_k, k = 2, 3, 4$, after [12]) are distinct ellipses; see Figure 1. Our main results are:

- If a triangle center X_k is a fixed linear combination of bary- X_2 and orthocenter X_4 , its locus is an ellipse (co-discovered with A. Akopyan [1]). Experimentally, the reverse seems also true, though we do not prove it.
- Over the continuous family of said linear combinations, centers of said loci sweep a straight line.
- Over the family of parallel V_1V_2 , the elliptic locus of X_k is a family of ellipses which rigidly translate along a line passing through O , the center of \mathcal{E} .

Additionally, we study the family of elliptic loci of X_k with V_1 fixed over all V_2 on \mathcal{E} . We show that (i) the locus of their centers is an ellipse axis-aligned with \mathcal{E} , and that (ii) the external envelope to the locus family is invariant over V_1 . In particular, the external envelope of X_4 (resp. X_2 's) loci is an affine image of Pascal's Limaçon (a 1/3-sized copy of \mathcal{E}).

Related Work. In [17], an explicit derivation is given for the elliptic locus of the orthocenter for the same triangle family studied in this article. Dykstra et al. [3] derived equations for loci of triangle centers under triangle families with two vertices affixed to special points of the ellipse. Loci of triangle centers have been studied for alternative triangle families including: (i) Poristic triangles (those with fixed

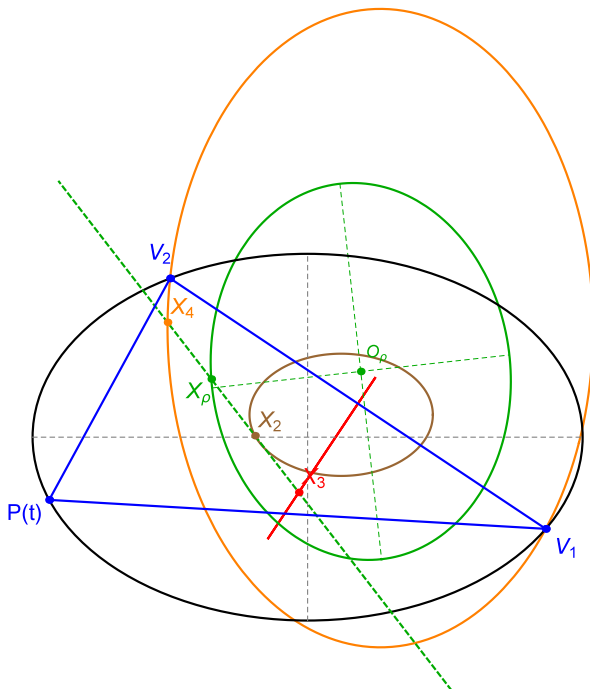


FIGURE 1. A triangle $V_1V_2P(t)$ (blue) is inscribed in an ellipse \mathcal{E} (black) with semi-axes a, b . While V_1, V_2 are fixed, $P(t)$ executes one revolution along the boundary. Consider triangle centers $X_k, k = 2, 3, 4$ on the Euler line \mathcal{L}_e (dashed green). For any choice of V_1V_2 , the locus of (i) X_2 is an axis-aligned ellipse (brown) with semi-axes $a/3, b/3$; (ii) X_3 is a segment (red) contained in the perp. bisector of V_1V_2 ; (iii) X_4 is an axis-aligned ellipse passing through V_1, V_2 , with aspect ratio b/a . An intermediate point X_ρ ($\rho = 1/2$) is shown on \mathcal{L}_e as well as its elliptic locus (green) centered on O_ρ . Though an ellipse for any ρ , this locus is in general neither axis-aligned (notice its slanted axes, dashed green), nor similar to \mathcal{E} . [Video](#)

incircle and circumcircle) [5, 29, 30, 19]. Odehnal describes pointwise, circular, and elliptic loci for dozens of triangle centers in the poristic family [20]. The poristic family is related via a similarity transform to another “famous” family: 3-periodics in the elliptic billiard [8]; (ii) triangles with common incircle and centroid. Pamfilos has shown their vertices lie on a conic [21]; (iii) Triangles with sides tangent to a circle [14]; (iv) Triangles associated with two lines and a point not on them [27], etc. (v) Stanev has describes the (ellptic) locus for the centroid of ellipse-inscribed equilaterals [28].

Some examples of polygon families include (i) rectangles inscribed in smooth curves [25], (ii) Poncelet polygons and the locus of their centroids [26] or their circumcenter [2].

We’ve studied loci of 3-periodics in the elliptic billiard, having found experimentally that the locus of the incenter is an ellipse [22]. This was subsequently proved [24]. Appearing thereafter were proofs for the elliptic locus of the barycenter [15] and circumcenter [4, 6]. More recently, with the help of a computer algebra system (CAS), we showed that 29 out of the first 100 entries in [12] are ellipses over billiard 3-periodics, though what determines ellipticity is still not understood [9]. We’ve

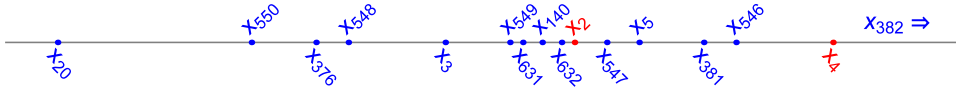


FIGURE 2. Relative locations of the first 16 triangle centers on [12] which are both on the Euler line and which are fixed linear combinations of X_2 and X_4 .

also studied properties (e.g., area invariance) of the negative pedal curve (NPC) of the ellipse with respect to a point on its boundary [10] as well as its pedal-like derivatives [23]. We have also studied the locus of Brocard points over circle- and ellipse-inscribed triangle families [7].

The envelope of Euler lines in triangles with two fixed vertices at the foci of an ellipse was studied in [16]. Note: we study loci of this family in Appendix C.

Article Structure. Section 2 defines basic concepts used in the article. Section 3 contains our main results. Section 4 analyzes loci over families of parallel V_1V_2 . Section 5 analyzes the envelope of loci with fixed V_1 and varying V_2 . In the conclusion, Section 6, a table is included with videos mentioned throughout the paper. A set of appendices is included: Appendix C overviews triangle centers whose loci are ellipses for a closely-related triangle family: V_1V_2 are fixed on the foci of \mathcal{E} . Appendix A includes longer calculations used in derivations of key properties of elliptic loci. Finally, Appendix D contains a quick-reference to most symbols used herein.

2. DEFINITIONS

Let (a, b) be the semi-axes of ellipse \mathcal{E} centered on O . Let $U(s) = [a \cos s, b \sin s]$ be a generic point on its boundary. Let t_1, t_2 be two constants, and define $V_1 = U(t_1)$, $V_2 = U(t_2)$. Consider the triangle family $\mathcal{T}(t) = V_1V_2P(t)$, where $P(t) = U(t)$, $t \in [0, 2\pi)$; see Figure 1.

Given a $\mathcal{T}(t)$, Let \mathcal{X}_ρ be a fixed linear combination of barycenter X_2 and orthocenter X_4 (both on Euler Line \mathcal{L}_e), i.e., $\mathcal{X}_\rho = (1 - \rho)X_2 + \rho X_4$; Figure 2 depicts the relative locations of the first 16 centers on [12] with fixed ρ , whereas Table 1 specifies their respective ρ .

X_k	20	550	376	548	3	549	631	140	632	2	547	5	381	546	4	382
ρ	-2	-1.25	-1	-0.875	-0.5	-0.25	-0.2	-0.125	-0.05	0	0.125	0.25	0.5	0.625	1	2.5

TABLE 1. First 16 points on [12] on Euler line and at fixed ρ .

Currently, upwards of 38k+ *triangle centers* are catalogued in [12]. These are points on the plane of a triangle whose trilinear (or barycentric) coordinates are functions of side lengths and angles. Said functions must satisfy homogeneity, bisymmetry, and cyclicity [31, Triangle Center]. Examples include such classic centers as the incenter X_1 , barycenter X_2 , circumcenter X_3 , orthocenter

Remark 1. Since \mathcal{X}_ρ is a linear combination of two triangle centers, its barycentrics add in a similar manner and therefore \mathcal{X}_ρ is also a triangle center [18].

Finally, let $c^2 = a^2 - b^2$, $d^2 = a^2 + b^2$, and $z = \cos(t_1 + t_2)$.

3. MAIN RESULTS

Referring to Figure 1:

Remark 2. Since $X_2 = [V_1 + V_2 + P(t)]/3$, the locus of X_2 is an ellipse \mathcal{E}_2 centered on $O_2 = (V_1 + V_2)/3$, axis-aligned with \mathcal{E} , and with semi-axes $(a_2, b_2) = (a/3, b/3)$.

Proposition 1. *For any V_1, V_2 , the locus of X_4 is an ellipse \mathcal{E}_4 of semi-axes a_4, b_4 , centered on O_4 , axis-aligned with \mathcal{E} , and with aspect ratio b/a . These are given by:*

$$O_4 = \frac{c^2}{2} \left[\frac{\cos t_1 + \cos t_2}{a}, \frac{\sin t_1 + \sin t_2}{b} \right]$$

$$(a_4, b_4) = (w/a, w/b), \quad \text{where: } w = \frac{\sqrt{2}}{2} \left(\sqrt{a^4 + b^4 + (b^4 - a^4)z} \right)$$

Proof. Using a CAS for simplification obtain the following parametric for \mathcal{E}_4 :

$$\begin{aligned} \mathcal{E}_4 : [x_4(t), y_4(t)], t \in [0, 2\pi), \text{ where:} \\ x_4(t) &= \frac{d^2(\cos t_1 + \cos t_2 + \cos t) + c^2 \cos(t_1 + t_2 + t)}{2a} \\ y_4(t) &= \frac{d^2(\sin t_1 + \sin t_2 + \sin t) + c^2 \sin(t_1 + t_2 + t)}{2b} \end{aligned}$$

□

Theorem 1. *For any V_1, V_2 , and any ρ , the locus of \mathcal{X}_ρ is an ellipse (in general not axis-aligned with \mathcal{E}) with parametric:*

$$\begin{aligned} \mathcal{E}_\rho : [x_\rho(t), y_\rho(t)], t \in [0, 2\pi), \text{ where:} \\ x_\rho &= \frac{(a^2(\rho + 2) + 3b^2\rho)(\cos t_1 + \cos t_2 + \cos t)}{6a} - \frac{c^2\rho \cos(t + t_1 + t_2)}{2a} \\ y_\rho &= \frac{(a^2(\rho + 2) + 3b^2\rho)(\sin t_1 + \sin t_2 + \sin t)}{6b} - \frac{c^2\rho \sin(t + t_1 + t_2)}{2b} \end{aligned}$$

and center O_ρ at:

$$O_\rho = \left[\frac{(a^2(\rho + 2) + 3b^2\rho)(\cos t_1 + \cos t_2)}{6a}, \frac{(3a^2\rho + b^2(\rho + 2))(\sin t_1 + \sin t_2)}{6b} \right]$$

Proof. CAS manipulation of $\mathcal{X}_\rho = (1 - \rho)X_2 + \rho X_4$. □

in Appendix B we've included all 226 triangle centers on [12] which are fixed linear combinations of X_2, X_4 .

As before, let $U(s)$ denote $[a \cos s, b \sin s]$ on \mathcal{E} .

Lemma 1. *Lines $U(t_1)U(t_2)$ are parallel for all $t_1 + t_2 = t_0$, where t_0 is some constant.*

Proof. The slope of the line through points $U(t_1) = [a \cos(t_1), b \sin(t_1)]$ and $U(t_2) = [a \cos(t_2), b \sin(t_2)]$ is given by

$$\frac{b(\sin t_1 - \sin t_2)}{a(\cos t_1 - \cos t_2)} = \frac{2b \cos(\frac{t_1+t_2}{2}) \sin(\frac{t_1-t_2}{2})}{-2a \sin(\frac{t_1+t_2}{2}) \sin(\frac{t_1-t_2}{2})} = -\frac{b}{a} \cot\left(\frac{t_0}{2}\right)$$

which only depends on t_0 . \square

Remark 3. Lemma 1 implies that if V_1V_2 are vertical (resp. horizontal), then $t_1 + t_2 = 2k\pi$ (resp. $t_1 + t_2 = (2k + 1)\pi$), where k is an integer.

Corollary 1. *For V_1V_2 vertical or horizontal, for all ρ , the locus of \mathcal{X}_ρ is axis-parallel with \mathcal{E} .*

Proof. Follows from the implicit equation for \mathcal{X}_ρ (Appendix A). Specifically, the coefficient a_{11} of xy vanishes whenever $t_1 + t_2$ is an integer multiple of π . \square

Let (a_ρ, b_ρ) denote the semi-axes of the locus of \mathcal{X}_ρ .

Proposition 2. *The ratio a_ρ/b_ρ is invariant over the family of parallel V_1V_2 .*

Proof. Rewrite the ellipse in Theorem 1 implicitly, and using a CAS obtain the ratio of eigenvalues of its Hessian, yielding the expression for a_ρ/b_ρ in Appendix A. Notice its non-constant terms only depend on the sum $t_1 + t_2$ which with Lemma 1 yields the claim. \square

Corollary 2. *For exactly three values of ρ , namely, $0, 1/4, 1$ (corresponding to X_2, X_5 , and X_4), the aspect ratio of the corresponding elliptic locus is independent of V_1 and V_2 , i.e., it only depends on (a, b) .*

Proof. For $\rho \in \{0, 1/4\}$ the aspect ratio is equal to a/b and for $\rho = 1/4$ it is equal to $(a^2 + b^2)/(2ab)$. From Appendix A it follows that $\lambda_\rho = a_\rho/b_\rho$ is a function of $[\rho, \cos(t_1 + t_2)] = (\rho, z)$. The function $\lambda_\rho(\rho, z)$ is independent of z when the level set $\partial\lambda_\rho/\partial z = 0$ is a vertical straight line. Direct analysis shows that is the case exactly when $\rho \in \{0, 1/4, 1\}$. \square

Proposition 3. *The product $a_\rho b_\rho$ is invariant over the family of parallel V_1V_2 and given by:*

$$a_\rho b_\rho = \frac{|(2\rho + 1)(2a^2b^2(\rho - 1) + 3\rho(a^4 - b^4)\cos(t_1 + t_2) - 3\rho(a^4 + b^4))|}{18ab}$$

Proof. Obtain the above from Equation 1 in Appendix A. Since for parallel V_1V_2 , $t_1 + t_2$ is constant (Lemma 1), the proof is complete. Alternatively, the same result could be obtained by symbolic simplification of the affine curvature of \mathcal{X}_ρ equal to $(a_\rho b_\rho)^{-2/3}$, since it is an ellipse [11]. \square

Remark 4. Only for $\rho \in \{0, -1/2\}$, i.e., $\mathcal{X}_\rho \in \{X_2, X_3\}$, is the product $a_\rho b_\rho$ independent of V_1V_2 , and equal to $ab/9$ and 0 , respectively.

Corollary 3 (Axis annihilation). *For each family of parallel V_1V_2 , there is a unique ρ (other than $-1/2$) such that the product $a_\rho b_\rho = 0$. Said ρ is given by:*

$$\rho = \frac{2a^2b^2}{3(a^4 - b^4)\cos(t_1 + t_2) + 2a^2b^2 - 3a^4 - 3b^4}$$

except when the denominator vanishes, which can only happen if $a/b < \sqrt{3}$. In this case, no ρ exists.

Proof. Follows from the expression for $a_\rho b_\rho$ in Proposition 3. \square

Remark 5. It $a/b = \sqrt{3}$, for vertical V_1V_2 , the axis can't be annihilated.

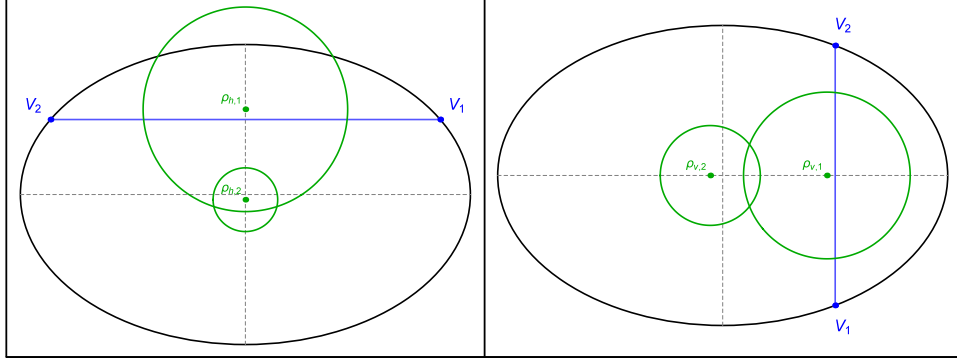


FIGURE 3. The loci of \mathcal{X}_ρ (green) can only be circles when V_1V_2 (blue) are horizontal (left) or vertical (right). When horizontal (resp. vertical) only at $\rho = \{\rho_{h,1}, \rho_{h,2}\}$ (resp. $\rho = \{\rho_{v,1}, \rho_{v,2}\}$) is the locus a circle. As the V_1V_2 traverse all horizontals (resp. verticals), the circles will rigidly translate vertically (resp. horizontally). [Video](#)

Referring to Figure 4:

Corollary 4. *The semi-axis lengths a_ρ, b_ρ of the locus of \mathcal{X}_ρ are invariant over the family of parallel V_1V_2 .*

Proof. By Proposition 2 and Lemma 3, the ratio a_ρ/b_ρ and product $a_\rho b_\rho$ of the axes are invariant over parallel V_1V_2 , respectively. The result follows. \square

Referring to Figure 3:

Proposition 4. *The locus of \mathcal{X}_ρ is a circle iff V_1V_2 is (i) horizontal with ρ assuming two values ρ_h , or (ii) vertical with $a \neq 3b$, and ρ assuming two values ρ_v . These are given by:*

$$\rho_h = \frac{b}{b \pm 3a}, \quad \rho_v = \frac{a}{a \pm 3b}$$

Proof. The parametrization for (x_ρ, y_ρ) in Theorem 1 can be developed to yield:

- For $t_1 + t_2 = \pi$ and $\rho = b/(b + 3a)$, \mathcal{X}_ρ is a circle centered in $[0, (a + b)^2 \sin t_1 / (3a + b)]$ and radius $a(a + b)/(b + 3a)$.
- For $t_1 + t_2 = \pi$ and $\rho = b/(b - 3a)$, \mathcal{X}_ρ is a circle centered in $[0, (a - b)^2 \sin t_1 / (b - 3a)]$ and radius $a(a - b)/(3a - b)$.
- For $t_1 + t_2 = 0$ and $\rho = a/(a + 3b)$, \mathcal{X}_ρ is a circle centered in $[(a + b)^2 \cos t_1 / (a + 3b), 0]$ and radius $b(a + b)/(a + 3b)$.
- For $t_1 + t_2 = 0$, $\rho = a/(a - 3b)$ and $a \neq 3b$, \mathcal{X}_ρ is a circle centered in $[(a - b)^2 \cos t_1 / (a - 3b), 0]$ and radius $|b(a - b)/(a - 3b)|$.

If V_1V_2 is neither horizontal nor vertical, there are no real solutions for ρ such that $a_\rho/b_\rho = 1$. \square

Proposition 5. *For V_1V_2 vertical, consider the case of $a = 3b$ and $\rho \notin \{-1/2, 3/2\}$. The locus of \mathcal{X}_ρ is the axis-aligned ellipse centered at $[2b(2r+3) \cos t_1/2, 0]$ and axes $a_\rho = b|2r-3|/3$, $b_\rho = b|2r+1|/3$. This ellipse is a circle when $\rho = 1/2$, i.e., when $\mathcal{X}_\rho = \mathcal{X}_{381}$.*

Proof. Direct derivation from Theorem 1. \square

Remark 6. By definition, X_3 is contained in the perpendicular bisector of V_1V_2 , given by:

$$-2a \sin(t_1 + t_2)x + 2b(\cos(t_1 + t_2) + 1)y + c^2(\cos t_1 + \cos t_2) \sin(t_1 + t_2) = 0$$

Proposition 6. *The locus of X_3 is a variable-length segment $P_3P'_3$ given by:*

$$\begin{aligned} P_{3,x} &= \frac{c^2}{4a} \left(\frac{(1 - \cos(2t_1 + 2t_2))}{\sqrt{2 - 2 \cos(t_1 + t_2)}} + \cos t_1 + \cos t_2 \right) \\ P_{3,y} &= -\frac{c^2}{4b} \left(\sqrt{2 - 2 \cos(t_1 + t_2)} + \sin t_1 + \sin t_2 \right) \\ P'_{3,x} &= \frac{c^2}{4a} \left(\frac{(\cos(2t_1 + 2t_2) - 1)}{\sqrt{2 - 2 \cos(t_1 + t_2)}} + \cos t_1 + \cos t_2 \right) \\ P'_{3,y} &= \frac{c^2}{4b} \left(\sqrt{2 - 2 \cos(t_1 + t_2)} - \sin t_1 - \sin t_2 \right) \end{aligned}$$

Furthermore, its length L_3 is given by:

$$L_3 = |P_3 - P'_3| = \frac{c^2 \sqrt{2(d^2 - c^2 \cos(t_1 + t_2))}}{2ab}$$

Proof. The coordinates of $X_3 = [x_3, y_3]$ are given by:

$$\begin{aligned} x_3 &= \frac{c^2}{4a} (\cos(t + t_1 + t_2) + \cos t_1 + \cos t_2 + \cos t) \\ y_3 &= \frac{c^2}{4b} (\sin(t + t_1 + t_2) - \sin t_1 - \sin t_2 - \sin t) \end{aligned}$$

Direct calculations yield the claimed expressions. \square

Corollary 5. *The min (resp. max) of L_3 is c^2/a (resp. c^2/b) and the midpoint of $P_3P'_3$ is given by*

$$\left[\frac{c^2}{4a} (\cos t_1 + \cos t_2), -\frac{c^2}{4b} (\sin t_1 + \sin t_2) \right]$$

Proof. Direct from the Proposition 6. \square

4. LOCUS CENTER TRANSLATION

Referring to Figure 4:

Proposition 7. *Over the family of parallel V_1V_2 , the locus of \mathcal{X}_ρ is a family of rigidly-translating ellipses whose center moves along a straight line \mathcal{L}_\parallel passing through O and given by:*

$$\mathcal{L}_\parallel : y = \frac{a}{b} \cdot \frac{(3a^2 + b^2)\rho + 2b^2}{(a^2 + 3b^2)\rho + 2a^2} \tan\left(\frac{t_1 + t_2}{2}\right) x$$

Proof. Directly from the expression for O_ρ in Theorem 1. \square

Remark 7. \mathcal{L}_\parallel is perpendicular to V_1V_2 when $\rho = 1$ (X_4).

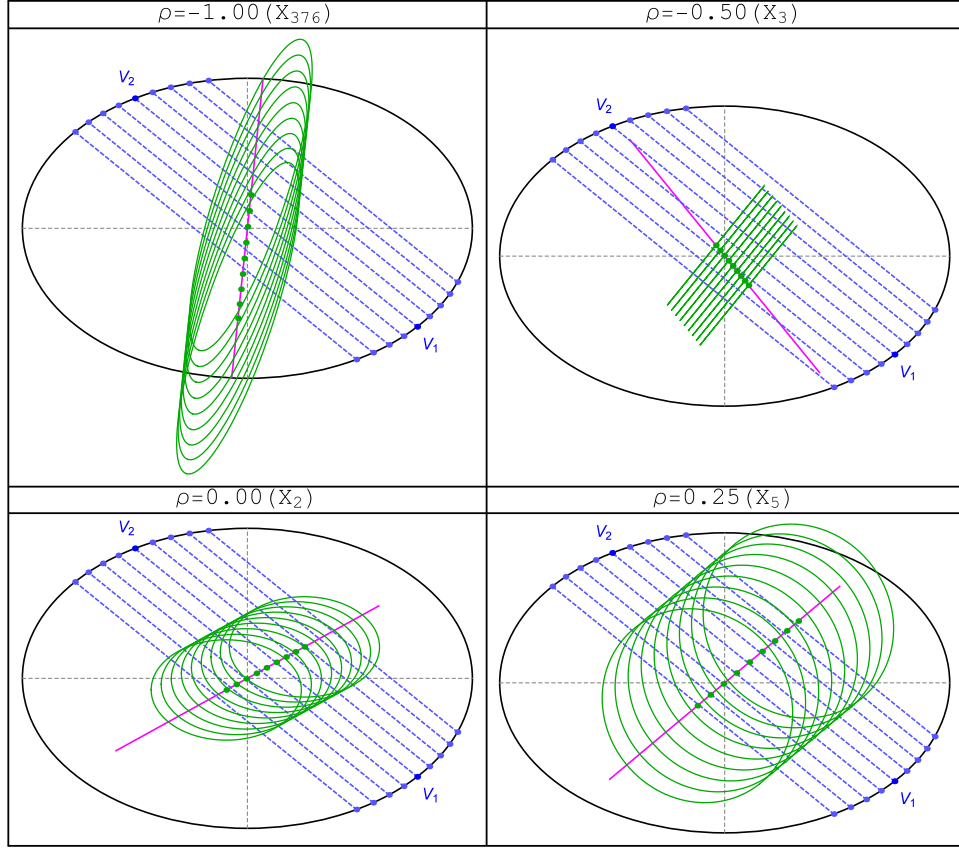


FIGURE 4. Over the family of parallel V_1V_2 (dashed blue, constant $t_1 + t_2$), the loci of \mathcal{X}_ρ (solid green) are a family of rigidly-translated ellipses. Their centers (green dots) move along a straight line \mathcal{L}_\parallel (magenta) which crosses \mathcal{E} 's center. Shown are the cases for $\rho \in \{-1, -1/2, 0, 1/4\}$, i.e., $X_k, k = 376, 3, 2, 5$, respectively. [Video](#)

Referring to Figure 5:

Proposition 8. *For V_1V_2 stationary, as one varies ρ , the center O_ρ of the locus of \mathcal{X}_ρ follows a straight line \mathcal{L}_ρ whose slope only depends on the slope of V_1V_2 . In fact:*

$$\mathcal{L}_\rho : \left[\frac{a(\cos t_1 + \cos t_2)}{3}, \frac{b(\sin t_1 + \sin t_2)}{3} \right] + \rho \cos\left(\frac{t_1 - t_2}{2}\right) \left[\frac{a^2 + 3b^2}{3a} \cos\left(\frac{t_1 + t_2}{2}\right), \frac{3a^2 + b^2}{3b} \sin\left(\frac{t_1 + t_2}{2}\right) \right]$$

Proof. Follows from Theorem 1. \square

Corollary 6. *The product of the slopes of \mathcal{L}_ρ and V_1V_2 is constant over all choices of V_1 and V_2 and equal to $-\frac{3a^2 + b^2}{a^2 + 3b^2}$.*

Corollary 7. *Only when V_1V_2 coincides with either the major or minor axis of \mathcal{E} can \mathcal{L}_ρ pass through the center of \mathcal{E} .*

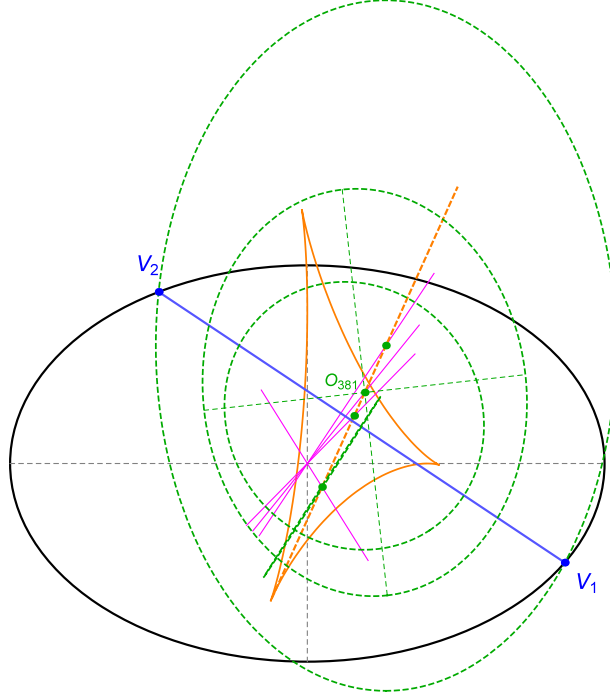


FIGURE 5. Elliptic loci (green ellipses) are shown for $\rho \in \{0, 1/4, 1/2, 1\}$ with centers $O_k, k = 2, 5, 381, 4$ on a line \mathcal{L}_ρ (dashed orange). Also shown is a family of lines \mathcal{L}_\parallel (magenta) passing through the center of \mathcal{E} depicting the locus of individual O_ρ as the family of parallel V_1V_2 is traversed. Also shown (solid orange) is the tricuspoid envelope of \mathcal{L}_ρ for fixed V_1 , over all V_2 on \mathcal{E} . [Video](#)

Referring to Figure 6 (bottom right):

Remark 8. When V_1V_2 passes thru O , \mathcal{L}_ρ collapses to O , and $O_\rho = O$ for all ρ .

Corollary 8. O_ρ is on V_1V_2 at the following ρ :

$$\rho = \frac{2a^2b^2}{3(b^4 - a^4)\cos(t_1 + t_2) + 2a^2b^2 + 3a^4 + 3b^4}$$

5. PHENOMENA WITH V_1 FIXED AND V_2 VARIABLE

5.1. **Envelope of \mathcal{L}_ρ .** Referring to Figure 5:

Proposition 9. For fixed V_1 , over all V_2 on \mathcal{E} , the envelope of \mathcal{L}_ρ is a deltoid-like curve Δ (with 3 cusps), given parametrically by:

$$\begin{aligned} \Delta_{t_1}(u) = & \left[\frac{\cos t_1 (a^4 - b^4)}{2a(3a^2 + b^2)}, -\frac{\sin t_1 (a^4 - b^4)}{2b(a^2 + 3b^2)} \right] \\ & + \left[\frac{(2 \cos u + \cos(t_1 + 2u))(a^4 - b^4)}{2a(3a^2 + b^2)}, -\frac{(2 \sin u - \sin(t_1 + 2u))(a^4 - b^4)}{2b(a^2 + 3b^2)} \right] \end{aligned}$$

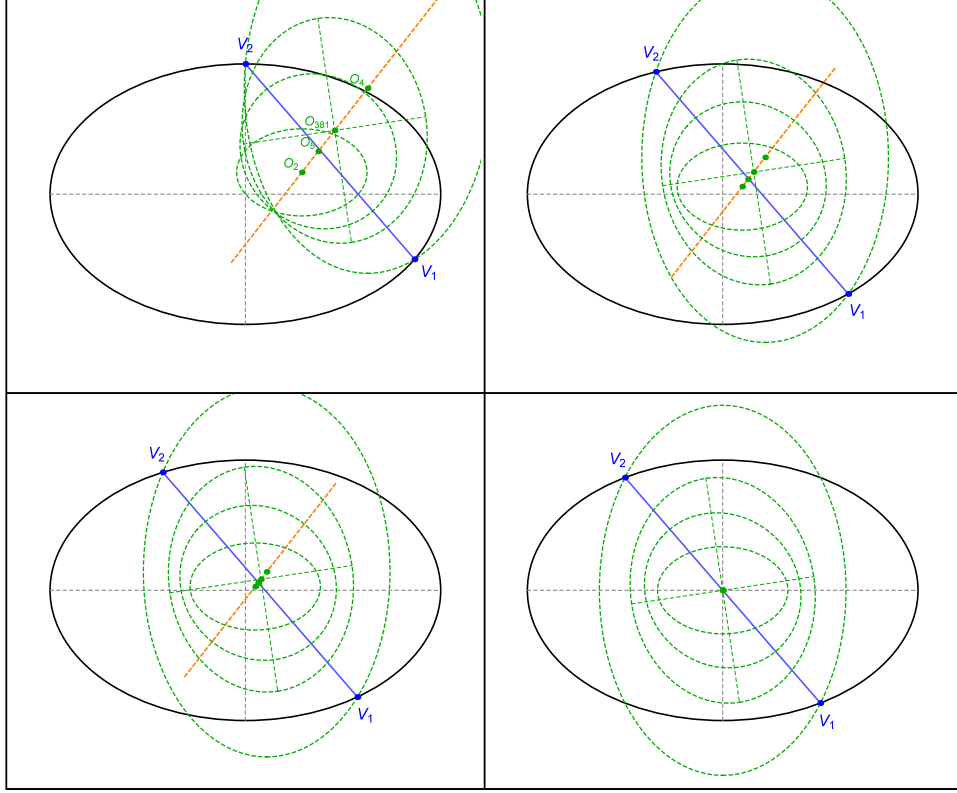


FIGURE 6. Four positions of parallel V_1V_2 are shown, approaching the center of \mathcal{E} . For each position, loci for $\rho = \{0, 1/4, 1/2, 1\}$ are collinear on \mathcal{L}_ρ (dashed orange). Notice as V_1V_2 approaches the position where it crosses the origin, centers come closer to each other and \mathcal{L}_ρ degenerates to a point (bottom right). [Video](#)

Proof. Follows from Proposition 8 and the definition of the envelope [11, Chapt. 3]. \square

Proposition 10. *The area of the region bounded by Δ_{t_1} is invariant over t_1 and given by*

$$A(\Delta_{t_1}) = \frac{\pi(a^4 - b^4)^2}{ab(3a^2 + b^2)(a^2 + 3b^2)}$$

5.2. **Locus of O_ρ .** Referring to Figure 7:

Proposition 11. *With V_1 fixed, over all V_2 , the locus of centers O_ρ of the loci of \mathcal{X}_ρ is an ellipse Γ_ρ centered on O'_ρ , which is axis-aligned with \mathcal{E} and contains its center O . Its semiaxes (a', b') and center are given by:*

$$(a', b') = \left(\frac{a^2(\rho + 2) + 3b^2\rho}{6a}, \frac{3a^2\rho + b^2(\rho + 2)}{6b} \right)$$

$$O'_\rho = [a' \cos t_1, b' \sin t_1]$$

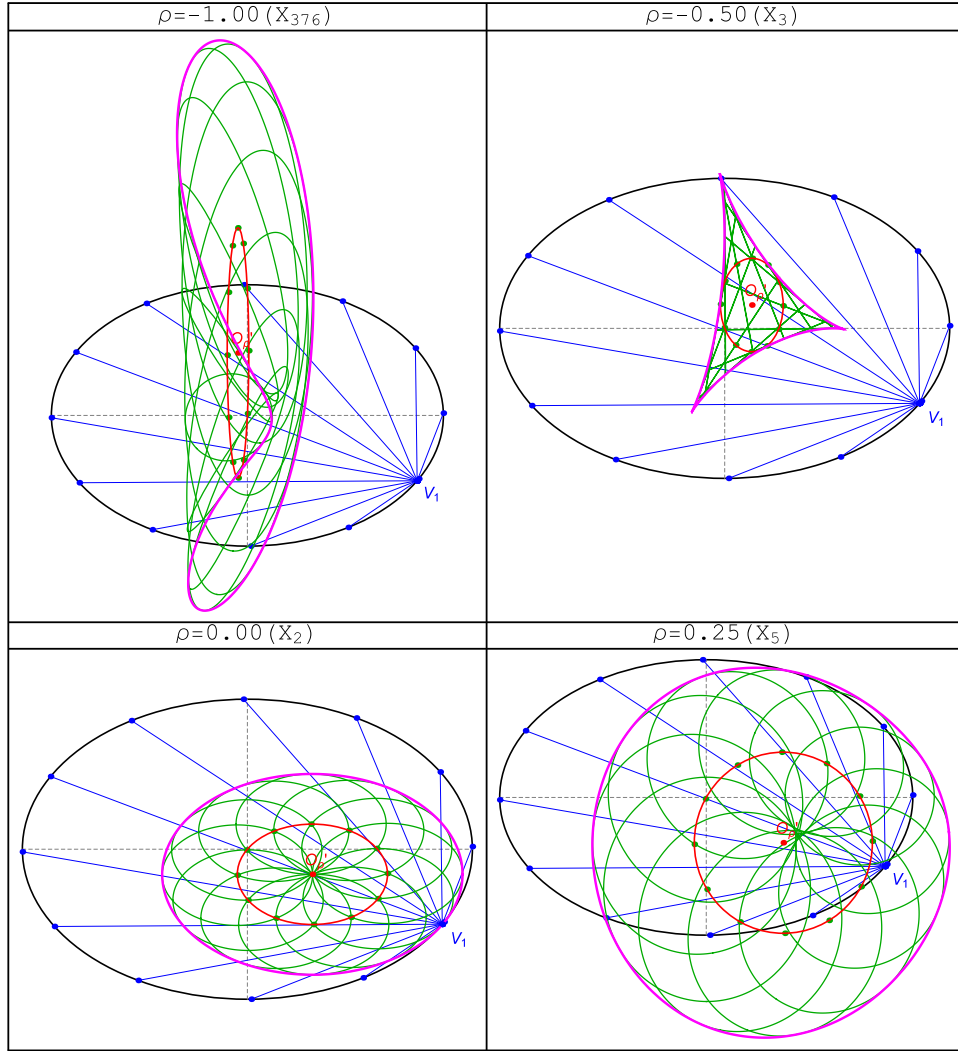


FIGURE 7. For a choice of V_1 and over V_2 on \mathcal{E} (black), the loci of X_ρ are a family of ellipses (green) whose centers (green dots) sweep an ellipse Γ_ρ passing through the center of \mathcal{E} and centered O'_ρ . Shown are the cases for $\rho \in \{-1, -1/2, 0, 1/4\}$, i.e., X_k , $k = 376, 3, 2, 5$, respectively. Also shown are envelopes (pink) to the ellipse families. For X_3 (top right), the envelope is a half-sized Steiner's hat [10]; for X_2 (bottom left) the envelope is an ellipse of fixed axes, internally tangent to \mathcal{E} at one point. All envelopes are area-invariant wrt V_1 .

Corollary 9. At $\rho = 1$ (X_4), Γ_ρ is an axis-aligned ellipse with aspect ratio b/a with center at $\left[\frac{(a^2+b^2)\cos t_1}{2a}, \frac{(a^2+b^2)\sin t_1}{2b} \right]$ and axes $(\frac{a^2+b^2}{2a}, \frac{a^2+b^2}{2b})$.

Corollary 10. At $\rho = 0$ (X_2), Γ_ρ is an ellipse with aspect ratio a/b centered at $[\frac{1}{3}a \cos t_1, \frac{1}{3}b \sin t_1]$ with axes $(\frac{a}{3}, \frac{b}{3})$.

Corollary 11. Over all V_1 the locus of O'_ρ is an ellipse Γ'_ρ which is axis-aligned and concentric with \mathcal{E} . The semi-axes of Γ'_ρ are also (a', b') .

Referring to Figure 8:

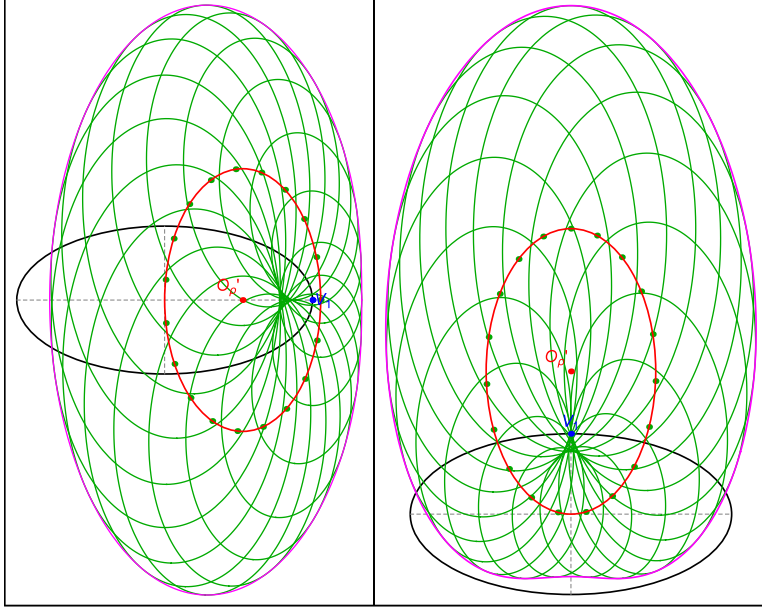


FIGURE 8. Locus Γ_ρ (red) of the centers of \mathcal{X}_ρ (green) of \mathcal{X}_ρ for $\rho = 2/3$, when V_1 coincides with the left (resp. top) vertex of \mathcal{E} (black). Notice Γ_ρ (red) is tangent at the center of O to the minor (resp. major) axis of \mathcal{E} and its center O'_ρ lies on the major (resp. minor) axis of \mathcal{E} .

Remark 9. If V_1 is fixed at the left (resp. top) vertex of \mathcal{E} , over all V_2 , Γ_ρ is axis-aligned with \mathcal{E} and tangent at O to its minor (resp. major) axis.

5.3. Envelope of the family of elliptic \mathcal{X}_ρ .

Proposition 12. *With V_1 stationary and V_2 sweeping the boundary of \mathcal{E} , a regular part of the envelope of \mathcal{X}_ρ is a curve Γ_{t_1} parametrized by*

$$x_{t_1} = \frac{[(a^2 + 3b^2)(2 \cos t + \cos t_1) - 3c^2 \cos(t_1 + 2t)] \rho}{6a} + \frac{a}{3} (2 \cos t + \cos t_1)$$

$$y_{t_1} = \frac{[(3a^2 + b^2)(2 \sin t + \sin t_1) - 3c^2 \sin(t_1 + 2t)] \rho}{6b} + \frac{b}{3} (2 \sin t + \sin t_1)$$

Proof. Direct from the definition of an envelope [11] via CAS simplification. \square

Proposition 13. *The area (algebraic) of the region bounded by Γ_{t_1} is invariant over t_1 and given by*

$$A(\Gamma_{t_1}) = \frac{\pi}{9} \left[\frac{(15a^4 + 2a^2b^2 + 15b^4) \rho^2}{2ab} + \frac{2(3a^4 + 2a^2b^2 + 3b^4) \rho}{ab} + 4ab \right]$$

Proof. Follows by direct integration of $A(\Gamma_{t_1}) = \frac{1}{2} \int_{\Gamma_{t_1}} (xdy - ydx)$. \square

In [10] we called *Steiner's Hat* the negative pedal curve of an ellipse with respect to a point M on the boundary. One of its curious properties is that it is area-invariant over all M .

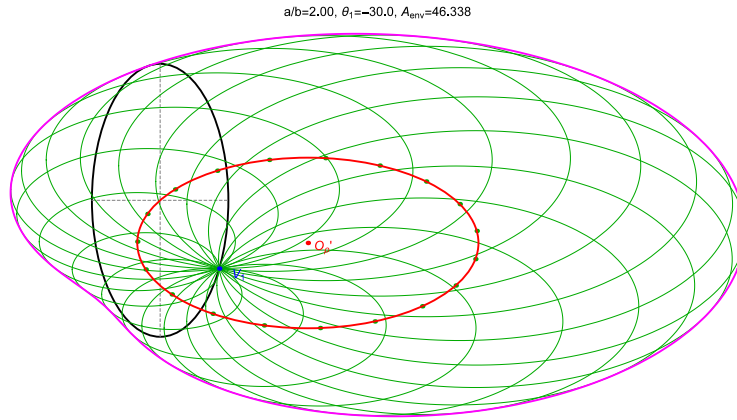


FIGURE 9. Let V_1 be a point on \mathcal{E} (black, rotated 90 degrees to save space, $a/b = 2$). Over V_2 , the loci of X_4 are ellipses (green) which all pass through V_1 . Their centers (green dots) sweep an axis-aligned ellipse (red) centered at O_ρ , whose aspect ratio is b/a . The exterior envelope of said loci is (in general) a non-convex curve (pink) which is the affine image of Pascal's Limaçon. Its area is independent of V_1 , and it is tangent to \mathcal{E} at at least one point. [Video](#)

Remark 10. With V_1 stationary and V_2 sweeping the boundary of \mathcal{E} , the envelope of the locus of X_3 over all positions of V_2 is 2:1 homothetic to Steiner's Hat.

This stems from the fact that it cuts V_1V_2 perpendicularly and at its midpoint. Referring to Figure 7 (bottom left) and Figure 9:

Remark 11. For $\rho = 0$ (resp. $\rho = 1$), the external envelope of \mathcal{X}_ρ is internally (resp. externally) tangent to \mathcal{E} at V_1 (resp. at the point(s) on \mathcal{E} whose normal goes through V_1). For $\rho = 0$ the envelope is elliptic with axes $2a/3$ and $2b/3$.

Proposition 14. *For $\rho = 1$, the external envelope of \mathcal{X}_ρ is the affine image of Pascal's Limaçon.*

Proof. A construction for Pascal's Limaçon is given in [31, Pascal's Limaçon] as follows: specify a fixed point P and a circle C . Then draw all circles with centers on C which pass through P . The external envelope of said circles is the Limaçon. Referring to Figure 9, apply an affine transformation that sends Γ_ρ to a circle C . This will automatically send all \mathcal{X}_ρ ellipses to (variable radius) circles, since they have the same aspect ratio and are axis-aligned with Γ_ρ (Proposition 11). Therefore, the affine image of the \mathcal{X}_ρ becomes a family of circles with centers on C through a common point P , the affine image of V_1 . \square

6. CONCLUSION

This article studied properties of the loci of triangle centers over of a special of ellipse-inscribed triangles. The following questions are still unanswered:

- Is there a triangle center which is not a fixed linear combination of X_2, X_4 whose locus over $\mathcal{T}(t)$ is an ellipse? We did not find one amongst all 38k+ centers listed in [12].
- For V_1 fixed and over all V_2 on \mathcal{E} , are there interesting properties of the internal envelope of the family of \mathcal{X}_ρ ellipses? For X_2, X_4 , this envelope is a point $(O + (V_1 - O)/3)$, and V_1 , respectively. However for other ρ this envelope is more complex.

Animations illustrating the dynamic geometry of some of the above phenomena appear on Table 2.

Id	Title	youtu.be/. . .
01	Basic elliptic loci	zjiNgfndBWg
02	\mathcal{X}_ρ slides on Euler line	w5KuN_OrQBQ
03	Locus of \mathcal{X}_ρ over parallel V_1V_2	zFOeENDJRho
04	Relative motion of loci over parallel V_1V_2	TpBjKlkFjkg
05	Circular loci if V_1V_2 are horiz. or vert.	nLeKvxcicNY
06	Limaçon-Like envelopes of X_4 locus family	sPQrz7ddRfA

TABLE 2. Illustrative animations, click on the link to view it on YouTube and/or enter `youtu.be/<code>` as a URL in your browser, where `<code>` is the provided string.

We are very grateful to A. Akopyan and P. Moses for key insights. We thank P.N. de Souza for his crucial editorial help. The second author is fellow of CNPq and coordinator of Project PRONEX/ CNPq/ FAPEG 2017 10 26 7000 508.

APPENDIX A. AXIS RATIO OF LOCUS OF \mathcal{X}_ρ

Here we assume the origin is at the center of the \mathcal{X}_ρ locus. Then the latter can be expressed as:

$$\mathcal{X}_\rho : a_{20}x_1^2 + 2a_{11}x_1y_1 + a_{02}y_1^2 + a_{00} = 0$$

The aspect ratio is given by:

$$\frac{a_\rho}{b_\rho} = \frac{a_{20} + a_{02} + \sqrt{(a_{20} - a_{02})^2 + 4a_{11}^2}}{2(a_{20}a_{02} - a_{11}^2)}$$

The product of axes is given by:

$$(1) \quad a_\rho b_\rho = \frac{|a_{00}|}{\sqrt{a_{20}a_{02} - a_{11}^2}}$$

where (recall $z = \cos(t_1 + t_2)$):

$$\begin{aligned} a_{20} &= 54a^2\rho c^2(3a^2\rho + b^2\rho + 2b^2)z \\ &\quad - 18a^2(9a^4 - 6b^2a^2 + 5b^4)\rho^2 - 36a^2b^2(3a^2 + b^2)\rho - 36a^2b^4 \\ a_{11} &= 54\rho(\rho - 1)abc^4\sqrt{1 - z^2} \\ a_{02} &= 54b^2\rho c^2(a^2\rho + 3b^2\rho + 2a^2)z \\ &\quad - 18b^2(5a^4 - 6b^2a^2 + 9b^4)\rho^2 - 36b^2(a^2 + 3b^2)a^2\rho - 36b^2a^4 \\ a_{00} &= (2\rho + 1)^2(3a^4\rho z - 3b^4\rho z - 3a^4\rho + 2a^2b^2\rho - 3b^4\rho - 2b^2a^2)^2 \end{aligned}$$

APPENDIX B. TRIANGLE CENTERS AT FIXED ρ

Amongst the 4.9k triangle centers on the Euler line [13], only the following 226 are fixed linear combinations of X_2 and X_4 : $X_k, k = 2, 3, 4, 5, 20, 140, 376, 381, 382, 546, 547, 548, 549, 550, 631, 632, 1564, 1656, 1657, 2041, 2042, 2043, 2044, 2045, 2046, 2675, 2676, 3090, 3091, 3146, 3522, 3523, 3524, 3525, 3526, 3528, 3529, 3530, 3533, 3534, 3543, 3545, 3627, 3628, 3830, 3832, 3839, 3843, 3845, 3850, 3851, 3853, 3854, 3855, 3856, 3857, 3858, 3859, 3860, 3861, 5054, 5055, 5056, 5059, 5066, 5067, 5068, 5070, 5071, 5072, 5073, 5076, 5079, 7486, 8703, 10109, 10124, 10299, 10303, 10304, 11001, 11539, 11540, 11541, 11737, 11812, 12100, 12101, 12102, 12103, 12108, 12811, 12812, 14093, 14269, 14782, 14783, 14784, 14785, 14813, 14814, 14869, 14890, 14891, 14892, 14893, 15022, 15640, 15681, 15682, 15683, 15684, 15685, 15686, 15687, 15688, 15689, 15690, 15691, 15692, 15693, 15694, 15695, 15696, 15697, 15698, 15699, 15700, 15701, 15702, 15703, 15704, 15705, 15706, 15707, 15708, 15709, 15710, 15711, 15712, 15713, 15714, 15715, 15716, 15717, 15718, 15719, 15720, 15721, 15722, 15723, 15759, 15764, 15765, 16239, 16249, 16250, 16446, 17504, 17538, 17578, 17800, 18585, 18586, 18587, 19708, 19709, 19710, 19711, 21734, 21735, 23046, 33699, 33703, 33923, 34200, 34551, 34552, 34559, 34562, 35018, 35381, 35382, 35384, 35400, 35401, 35402, 35403, 35404, 35405, 35406, 35407, 35408, 35409, 35410, 35411, 35412, 35413, 35414, 35415, 35416, 35417, 35418, 35419, 35420, 35421, 35434, 35435, 35732, 35734, 35735, 35736, 35737, 35738, 36436, 36437, 36438, 36439, 36445, 36448, 36454, 36455, 36456, 36457, 36463, 36466.$

APPENDIX C. FOCUS-MOUNTED TRIANGLES

Consider the 1d family of triangles $\mathcal{T}_f(t) = f_1 f_2 P(t)$ where $P(t)$ sweeps \mathcal{E} and the f_j are the foci of \mathcal{E} , at $[\pm c, 0]$. Referring to Figure 10, noting that the result for X_1, X_2 were proved in [3, Thm 2.2.1]:

Proposition 15. *Over the first 1000 triangle centers listed in [12], only the loci of $X_k, k = 1, 2, 8, 10, 145, 551$ over $\mathcal{T}_f(t)$ are ellipses. The first four are given by:*

$$\begin{aligned} X_1 &: \frac{x^2}{c^2} + \frac{(a+c)^2 y^2}{b^2 c^2} - 1 = 0 \\ X_2 &: \frac{9x^2}{a^2} + \frac{9y^2}{b^2} - 1 = 0 \\ X_8 &: \frac{x^2}{(a-2c)^2} + \frac{y^2 (a+c)^2}{b^2 (a-c)^2} - 1 = 0 \\ X_{10} &: \frac{4x^2}{(a-c)^2} + \frac{4(a+c)^2 y^2}{a^2 b^2} - 1 = 0 \end{aligned}$$

Remark 12. The vertices of the locus of X_1 are f_1, f_2 .

Remark 13. At $a = 2c$, i.e., $a/b = 2/\sqrt{3} \simeq 1.1547$, the locus of X_8 is the vertical segment $[0, \pm b/3]$. At this aspect ratio, when $P(t)$ is at the top or bottom vertex of \mathcal{E} , $\mathcal{T}_f(t)$ is equilateral.

Recall Line $X_1 X_2$ is known as the *Nagel Line* [13]. For the entire 40k+ centers in [12], the following 62 are fixed linear combinations of X_1, X_2 (boldface indicates those in Proposition 15): **1, 2, 8, 10, 145, 551**, 1125, 1698, 3241, 3244, 3616, 3617, 3621, 3622, 3623, 3624, 3625, 3626, 3632, 3633, 3634, 3635, 3636, 3679, 3828, 4668, 4669, 4677, 4678, 4691, 4701, 4745, 4746, 4816, 5550, 9780, 15808, 19862, 19872, 19875, 19876,

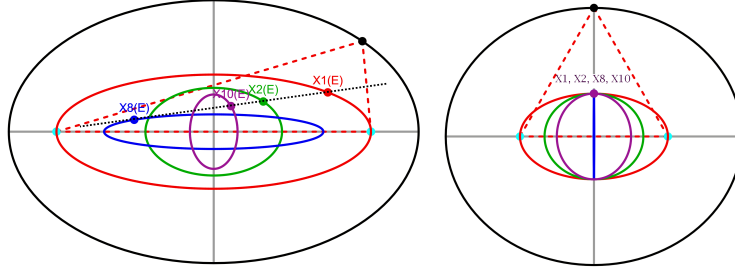


FIGURE 10. **Left:** elliptic loci of $X_k, k = 1, 2, 8, 10$ (collinear on the Nagel line, dashed black) for a triangle family (dashed red) with two vertices on the foci. [animation 1](#) **Right:** at $a/b = 2/\sqrt{3} \approx 1.1547$, the family contains two equilaterals (one shown dashed red), and therefore all loci are tangent at two point. Also at this a/b , the locus of X_8 (blue) is a vertical segment. [animation 2](#)

19877, 19878, 19883, 20014, 20049, 20050, 20052, 20053, 20054, 20057, 22266, 25055, 31145, 31253, 34595, 34641, 34747, 36440, 36444, 36458, 36462.

Note that X_2 is the anticomplement of itself. Note also that X_{10} (resp. X_{145}) is the anticomplement of X_1 (resp. X_8). Numerically analyzing the loci of all 38k+ on [12] which are not on the X_1X_2 line we found none which produced an ellipse over $\mathcal{T}_f(t)$. In turn this leads to the following conjecture:

Conjecture 1. *The locus of X_k over $\mathcal{T}_f(t) = f_1f_2P(t)$ is an ellipse iff X_k is a fixed linear combination of X_1 and X_2 .*

APPENDIX D. TABLE OF SYMBOLS

Symbols used in the article appear on Table 3.

symbol	meaning
\mathcal{E}, a, b	base ellipse and its semi-axes
O, f_1, f_2	center of foci of \mathcal{E}
V_1, V_2	points fixed on \mathcal{E} at t_1, t_2
$P(t)$	moving 3rd vertex of \mathcal{T}
$\mathcal{T}(t)$	\mathcal{E} -inscribed triangle $V_1V_2P(t)$
\mathcal{L}_e	Euler line X_2X_4
\mathcal{X}_ρ, ρ	$\mathcal{X}_\rho = X_2 + \rho(X_4 - X_2)$
c^2, d^2	$a^2 - b^2$, and $a^2 + b^2$, resp.
z	shorthand for $\cos(t_1 + t_2)$
O_ρ	center of elliptic locus of \mathcal{X}_ρ
$\mathcal{L}_\rho, \mathcal{L}_\parallel$	linear locus of O_ρ over ρ (resp. V_1V_2 parallels)
Δ_{t_1}	envelope of \mathcal{L}_ρ for fixed V_1 over V_2 on \mathcal{E}
Γ_ρ	elliptic locus of O_ρ for fixed V_1 over V_2 on \mathcal{E}
O'_ρ, Γ'_ρ	center of Γ_ρ and its elliptic locus over all V_1 on \mathcal{E}
X_1, X_2	incenter, barycenter
X_3, X_4	circumcenter, orthocenter
X_5, X_8	9-pt circle center and Nagel point
X_{10}, X_{381}	Spieker center and X_2X_4 midpoint

TABLE 3. Symbols used in the article.

REFERENCES

- [1] Akopyan, A. (2020). Locus of x_ρ is an ellipse if it lies on euler line at fixed linear combination of x_2, x_4 . Private Communication. 1
- [2] Chavez-Caliz, A. (2020). More about areas and centers of Poncelet polygons. *Arnold Math J.* doi.org/10.1007/s40598-020-00154-8. 2
- [3] Dykstra, J., Peterson, C., Rall, A., Shaddock, E. (2006). Orbiting vertex: Follow that triangle center! bit.ly/2JaWMK9. 1, 15
- [4] Fierobe, C. (2018). On the circumcenters of triangular orbits in elliptic billiard. arxiv.org/pdf/1807.11903.pdf. Submitted 2
- [5] Gallatly, W. (1913). *The Modern Geometry of the Triangle*. London: Hodgson. 2
- [6] Garcia, R. (2019). Elliptic billiards and ellipses associated to the 3-periodic orbits. *American Mathematical Monthly*, 126(06): 491–504. doi.org/10.1080/00029890.2019.1593087. 2
- [7] Garcia, R., Reznik, D. (2020). Loci of the brocard points over selected triangle families. <https://arxiv.org/abs/2009.08561>. ArXiv:2009.08561. 3
- [8] Garcia, R., Reznik, D. (2020). Related by similiarity: Poristic triangles and 3-periodics in the elliptic billiard. arxiv.org/abs/2004.13509. 2
- [9] Garcia, R., Reznik, D., Koiller, J. (2020). Loci of 3-periodics in an elliptic billiard: why so many ellipses? ArXiv:2001.08041. 2
- [10] Garcia, R., Reznik, D., Stachel, H., Helman, M. (2020). A family of constant-areas deltoid associated with the ellipse. *arXiv*. arxiv.org/abs/2006.13166. 3, 11, 12
- [11] Guggenheimer, H. (1977). *Differential Geometry*. New York: Dover. 5, 10, 12
- [12] Kimberling, C. (2019). Encyclopedia of triangle centers. faculty.evansville.edu/ck6/encyclopedia/ETC.html. 1, 2, 3, 4, 13, 15, 16
- [13] Kimberling, C. (2020). Central lines of triangle centers. bit.ly/34vVoJ8. 15
- [14] Kovačević, N., Šlipečević, A. (2012). On the certain families of triangles. *KoG-Zagreb*, 16: 21–27. 2
- [15] Levi, M., Tabachnikov, S. (2007). The Poncelet grid and billiards in ellipses. *The American Mathematical Monthly*, 114(10): 895–908. doi.org/10.1080/00029890.2007.11920482. 2
- [16] MacQueen, M. L., Hartley, R. W. (1946). Elliptic Euleroids. *Amer. Math. Monthly*, 53: 511–516. <https://doi.org/10.2307/2305067>. 3
- [17] Monroe, D., Blue (2019). Locus of orthocenter of triangle inscribed in ellipse. bit.ly/2T60qFh. Stack Exchange. 1
- [18] Moses, P. (2020). A linear combination of two triangle centers is a triangle center. Private Communication. 3
- [19] Murnaghan, F. D. (1925). Discussions: Note on Mr. Weaver’s paper “a system of triangles related to a poristic system” (1924, 337–340). *Amer. Math. Monthly*, 32(1): 37–41. www.jstor.org/stable/2300090. 2
- [20] Odehnal, B. (2011). Poristic loci of triangle centers. *J. Geom. Graph.*, 15(1): 45–67. 2
- [21] Pamfilos, P. (2011). Triangles with given incircle and centroid. *Forum Geometricorum*, 11: 27–51. 2
- [22] Reznik, D. (2011). The locus of the incenter over 3-periodics in the elliptic billiard is an ellipse. youtu.be/BSyM7RnswA. 2
- [23] Reznik, D., Garcia, R., Stachel, H. (2020). Area-invariant pedal-like curves derived from the ellipse. arxiv.org/abs/2009.02581. ArXiv:abs/2009.02581. 3
- [24] Romaskevich, O. (2014). On the incenters of triangular orbits on elliptic billiards. *Enseign. Math.*, 60(3-4): 247–255. arxiv.org/pdf/1304.7588.pdf. 2
- [25] Schwartz, R. (2019). Rectangle coincidences and sweepouts. arxiv.org/abs/1809.03070. 2
- [26] Schwartz, R., Tabachnikov, S. (2016). Centers of mass of Poncelet polygons, 200 years after. *Math. Intelligencer*, 38(2): 29–34. bit.ly/3kLetNU. 2
- [27] Šlipečević, A., Halas, H. (2013). Family of triangles and related curves. *Hrvat. Akad. Znan. Umjet. Mat. Znan*, 17(515): 203–2010. 2
- [28] Stanev, M. (2019). Locus of the centroid of the equilateral triangle inscribed in an ellipse. *International Journal of Computer Discovered Mathematics (IJCDM)*, 4. bit.ly/371XH4v. 2
- [29] Weaver, J. H. (1924). A system of triangles related to a poristic system. *Amer. Math. Monthly*, 31(7): 337–340. www.jstor.org/stable/2299387. 2
- [30] Weaver, J. H. (1933). Curves determined by a one-parameter family of triangles. *Amer. Math. Monthly*, 40(2): 85–91. www.jstor.org/stable/2300940. 2

- [31] Weisstein, E. (2019). Mathworld. *MathWorld—A Wolfram Web Resource*. mathworld.wolfram.com. 3, 13